

# Chattering Analysis of an Optimized Sliding Mode Controller for an Electro-Hydraulic Actuator System

Chong Chee Soon<sup>1</sup>, Rozaimi Ghazali<sup>2,\*</sup>, Muhamad Fadli Ghani<sup>3</sup>, Chai Mau Shern<sup>4</sup>, Yahaya Md. Sam<sup>5</sup>, Zulfatman Has<sup>6</sup>

<sup>1,2,3,4</sup>Centre for Robotics and Industrial Automation (CeRIA), Faculty of Electrical Engineering,  
Universiti Teknikal Malaysia Melaka, Hang Tuah Jaya, Durian Tunggal, Melaka, Malaysia

<sup>3</sup>Malaysian Institute of Marine Engineering Technology (MIMET),  
Universiti Kuala Lumpur, Lumut, Perak, Malaysia

<sup>5</sup>Department of Control and Mechatronics Engineering, School of Electrical Engineering,  
Universiti Teknologi Malaysia, Skudai, Johor, Malaysia

<sup>6</sup>Electrical Engineering Department, University of Muhammadiyah Malang, Malang, Indonesia

Email: <sup>1</sup> p011720001@student.utm.edu.my, <sup>2,\*</sup> rozaimi.ghazali@utm.edu.my, <sup>3</sup> muhamadfadli@unikl.edu.my, <sup>4</sup> maushern@gmail.com, <sup>5</sup> yahaya@fke.utm.edu.my, <sup>6</sup> zulfatman@umm.ac.id

\*Corresponding Author

**Abstract**—Wear and tear are usually caused by various factors, which reduce the life span of a mechanical part. In the control engineering of an electro-hydraulic actuator (EHA) system, the wear and tear can be caused by the system or the controller itself. This article mainly examines the chattering effect that occurs during the sliding mode controller (SMC) design and its effect on the nonlinear EHA system. To examine the chattering phenomenon, a signum function is first applied to the switching function of the SMC. Then, parameters of the controller are obtained using the particle swarm optimization (PSO) method through a single objective function. These parameters are then applied to the switching function with the hyperbolic tangent function. Lastly, the performances of both functions are analyzed and compared based on graph and numerical data. From the output data, the chattering phenomenon generated on the signum function is greatly eliminated by using the hyperbolic tangent function. Thus, it can be inferred that the performance of the SMC can be greatly enhanced by manipulating the formula of the switching function.

**Keywords**—Sliding mode control; Electro-hydraulic actuator (EHA); Chattering analysis

## I. INTRODUCTION

Common modern appliances are usually equipped with sensory devices that require manipulation of the control system [1]. Electro-hydraulic actuator (EHA) system is one of the example applications that is equipped with these technologies and implemented in various industrial processes [2]. Usually, the proportional-integral-and derivative (PID) controller is the widely seen controller in common industrial applications [3]–[5]. This controller required no thorough knowledge to execute some simple process [6]. Furthermore, the parameters of this controller can be easily obtained through the try and error method for the simple processes that high precision is not required [7]. An operator can easily tune the controller parameters manually as long as the work is done.

In a process that required long operating hours, the robustness of this controller required to be further examined

[8]. In addition, most of the real-life applications correspond to uncertainties and nonlinearities [9]–[11]. These properties are inherently existed and lead to the lifespan issue of the applications and directly affect the expenses [12]. Therefore, the PID controller becomes a favorite trademark among researchers in the development of more advanced control strategies [13]–[15]. One of the commonly known advanced control strategies is sliding mode control (SMC). This controller is well-known to be outperformed and implemented in various types of applications such as robotic [16]–[19], flight [20]–[23], and ship [24]–[27].

Dealing with the outperform performances, comprehensive knowledge about the characteristic of this SMC control is required [28]. With the great contribution of the mathematician, this SMC controller is upgraded from time to time. It is noted that the general structure of the SMC is a combination of the two phases, known as the sliding phase and reaching phase [29]–[31]. These two phases are the main elements that are required to be thoroughly understood to achieve the desired response. Thus, researchers are usually manipulating these two elements based on their control objective and application.

This article demonstrates the effect of two common functions applied on the switching control of the SMC. By applying a typical signum function on the switching phase, a clear effect can be observed by only replacing the signum function with a hyperbolic tangent function. Considered as a simple method that greatly enhances the understanding in the control performance, it subsequently demonstrates a great influence of mathematics on human life.

This article is organized with a common interpretation of the system and control design in the introduction section. The mathematical derivation of the controller design and the short explanation of the particle swarm optimization (PSO) tuning algorithm is explained in the second section. This is followed by the results and discussion of the article. Finally is the conclusion of the article.



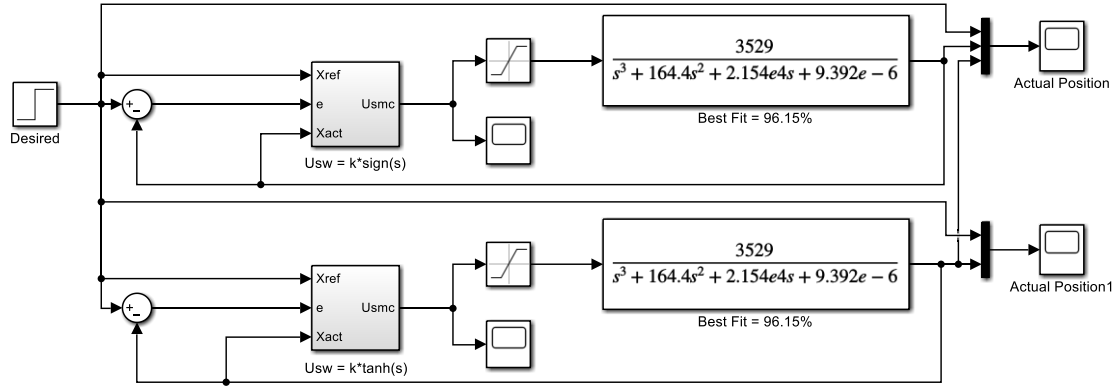


Fig. 1. Block diagram in tracking performances analyses.

## II. CONTROL AND TUNING

Fig. 1 represents the block diagram of this article where two functions of signum and hyperbolic tangent are compared based on tracking performance and their performance on the sliding surface.

The general sliding surface of SMC control is based on the equation as

$$s(t) = \left( \lambda + \frac{d}{dt} \right)^{n-1} e(t) \quad (1)$$

where  $\lambda$  is the coefficient of the sliding surface,  $n$  is the order of the system,  $e$  is the error.

An EHA system is a third-order model system [32] with the following sliding surface equation.

$$\begin{aligned} s(t) &= \left( \lambda + \frac{d}{dt} \right)^{3-1} e(t) \\ &= (\lambda^2 e(t) + 2\lambda \dot{e}(t) + \ddot{e}(t)) \end{aligned} \quad (2)$$

The general error equation is expressed as,  $e = X_{ref} - X_{act}$ , and the third-order error EHA system will lead to  $\ddot{e} = \ddot{X}_{ref} - \ddot{X}_{act}$ . Where  $e$  is the error,  $X_{ref}$  is the reference input position,  $X_{act}/X_p$  is the actual output position.

The first derivative of the sliding surface for the third-order EHA system is as below:

$$\dot{s}(t) = (\lambda^2 \dot{e}(t) + 2\lambda \ddot{e}(t) + \ddot{e}(t)) \quad (3)$$

Substituting Equation (2) into (3), the following equation is obtained.

$$\dot{s}(t) = (\lambda^2 \dot{e}(t) + 2\lambda \ddot{e}(t) + [\ddot{X}_{ref}(t) - \ddot{X}_{act}(t)]) \quad (4)$$

The transfer function based on the electro-hydraulic model in [33], obtained using system identification method with the highest best fit of 96.15% as depicted in Fig. 1, is given by

$$TF = \frac{X_p(s)}{U(s)} = \frac{3529}{s^3 + 164.4s^2 + 2.154^4s + 9.392^{-06}}$$

$$\ddot{X}_p = 3529U - 164.4\ddot{X}_p - 2.154^4\dot{X}_p - 9.392^{-06}X_p \quad (5)$$

where  $X_p = X_{act}$ , the actual position/actual output displacement of the EHA actuator. Thus, the sliding surface equation below formed.

$$\begin{aligned} \dot{s}(t) &= (\lambda^2 \dot{e}(t) + 2\lambda \ddot{e}(t) + \ddot{e}(t)) \\ &= (\lambda^2 \dot{e}(t) + 2\lambda \ddot{e}(t) + \ddot{X}_{ref} - 3529U_{eq} \cdots \\ &\quad + 164.4\ddot{X}_p + 2.154^4\dot{X}_p + 9.392^{-06}X_p) \end{aligned} \quad (6)$$

When the phases shift to the sliding surface where  $s(t) = \dot{s}(t) = \ddot{s}(t) \cdots = 0$  the equivalent control will lead the state to the desired response. Where  $U_{eq}$  can be formed as below:

$$\begin{aligned} 0 &= (\lambda^2 \dot{e}(t) + 2\lambda \ddot{e}(t) + \ddot{X}_{ref}(t) - 3529U_{eq} + \cdots \\ &\quad 164.4\ddot{X}_p + 2.154^4\dot{X}_p + 9.392^{-06}X) \\ U_{eq} &= \frac{1}{3529} (\lambda^2 \dot{e}(t) + 2\lambda \ddot{e}(t) + \ddot{X}_{ref}(t) + \cdots \\ &\quad 164.4\ddot{X}_p + 2.154^4\dot{X}_p + 9.392^{-06}X) \end{aligned} \quad (7)$$

In the reaching phase of the SMC,  $U_{sw}$  is responsible to leads the state to the sliding phase. Generally, the switching function of SMC is formed using the signum function as in Fig. 2 [34].

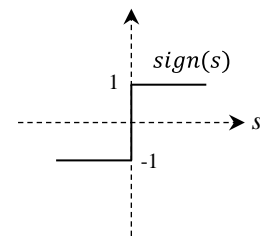


Fig. 2. The general structure of signum function.

It is defined where signum function is a function that takes the sign of a real number, either positive or negative, with the following definition.

$$\text{signum} = \begin{cases} 1 & \text{if } s > 0, \\ 0 & \text{if } s = 0, \\ -1 & \text{if } s < 0. \end{cases} \quad (8)$$

General switching control of the SMC that formed using signum function is expressed in (9) [35].

$$U_{sw} = k \operatorname{sign}(s) \quad (9)$$

To reduce the high dynamic switching on the signum function, a hyperbolic tangent switching as in Fig. 3 is introduced.

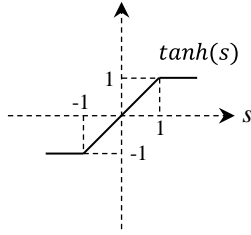


Fig. 3. The general structure of the hyperbolic tangent function.

Also known as relaxation of the gradient of signum function. Then, the switching function is expressed as:

$$U_{sw} = k \tanh(s) \quad (10)$$

The general structure of the SMC control consists of equivalent control,  $U_{eq}$  and switching control,  $U_{sw}$ .  $U_{eq}$  corresponding to the sliding phase when  $s(t) = 0$ , while  $U_{sw}$  It corresponds to the reaching phase when  $s(t) \neq 0$ .

$$U_{smc}(t) = U_{eq}(t) + U_{sw}(t) \quad (11)$$

Thus, by substituting the equation in (7) and (10) into (11), the sliding mode control,  $U_{smc}$  can be expressed as:

$$U_{smc}(t) = \frac{1}{3529} \left( \lambda^2 \dot{e}(t) + 2\lambda \ddot{e}(t) + \ddot{X}_{ref}(t) + \dots \right. \\ \left. 164.4 \ddot{X}_p + 2.154^{04} \dot{X}_p + 9.392^{-06} X \right) + \dots \quad (k \tanh(s)) \quad (12)$$

Discussion of the PSO algorithm can also be found in [32], where two important parameters of  $\lambda$  and  $k$  in SMC are affected by the variables of PSO, as listed in Table I. The objective function of Integral Absolute Error (IAE) has been applied in the tuning. If these values are implemented in the algorithm, random approximate values should be obtained. A uniform distribution formulation will be used to obtain the values within the lower bound and upper bound that represent the desired searching area.

### III. TRACKING ANALYSES

Analyses have been conducted by using the latest available MATLAB/Simulink 2021a software installed in a laboratory computer with an i7 computer processor. To simulate the particle swarm optimization algorithm, the Simulink model configuration must be adjusted to generate

the ‘Time (tout)’ parameter, which is generated in default from the oldest version MATLAB/Simulink software (2018 or earlier).

In examining the performance of signum and hyperbolic tangent functions on the switching control, the unit step desired value is applied. The final position of 0.03 meters, with a time interval of 0.001 seconds and the step time of 0.5 seconds, has been implemented in the desired values.

In the sliding mode controller (SMC), the analyses will be made on the switching function, as explained earlier. The switching function that applies the signum function in the suggestion of the previous literature will be replaced by the hyperbolic tangent function. Firstly, the switching gain of the signum function,  $k$  as in Equation (9), and the parameter of the SMC sliding surface,  $\lambda$ , are tuned using the particle swarm optimization (PSO) metaheuristic algorithm. Then, the signum function will be substituted by the hyperbolic tangent function as denoted in Equation (10). Similar parameters, 14.7310 and 0.0112, represent  $\lambda$  and  $k$  gains, respectively, will be applied in both functions.

Therefore, the effect of interchanging between these two functions can be monitored. An electrohydraulic model transfer function with 96.15% best fit obtained using the system identification method is examined.

Based on the simulation result in Fig. 4, the output tracking performance of the EHA system is better when the signum function is applied, based on the waveform pattern in the legend. Slight undershoot occurs in the early tracking of the hyperbolic tangent function. The situation that occurred is due to the tuning algorithm, where tuning is made for the Signum function. If the tuning is applied to the hyperbolic tangent function, a similar situation will occur where the hyperbolic tangent will perform better based on eyesight. Thus, the performances can be explained further by referring to percentage improvement and decrement, transient response, steady-state error, and root means square analyses, as listed in Table II. According to the numerical results obtained from these two functions as listed in the table, the performance of overshoot percentages, rise time, steady-state errors of the signum function is slightly higher than the hyperbolic tangent function in the time of three seconds. From a practical point of view, these analyses might not affect much when dealing with a real application that usually existed with delay circumstance.

However, in terms of steady-state errors, since it is varied over time, further inspection in an experimental analysis is necessary to avoid higher errors in a long time. As depicted in a zoomed Fig. 4, a slight chattering phenomenon is occurred visually due to the high dynamic switching feature of the sign function.

TABLE I. VALUE SETTING IN PSO ALGORITHM

Terms	Description	Values
$lb$	Lower (lower)	0
$ub$	Boundary (upper)	20
$p$	Number of particles, where $p = 1, 2, 3, \dots, n$	100
$d$	Problem dimension, where $d = 1, 2, 3, \dots, n$	100

TABLE II. TRANSIENT RESPONSE, STEADY-STATE ERROR, AND ROOT MEAN SQUARE ERROR

Switching Function	Transient Response			Steady-state Error ( $e_{ss}$ )	RMSE
	OS (%)	$T_r$ (s)	$T_s$ (s)		
sign	0.8246	0.0990	0.6567	$3.6132 \times 10^{-6}$	0.004180
tanh	0.2432	0.0988	0.8609	$3.0070 \times 10^{-11}$	0.004184
Improvement/ Decrement (%)	70.5069	0.2020	-23.7194	99.9992	-0.0956

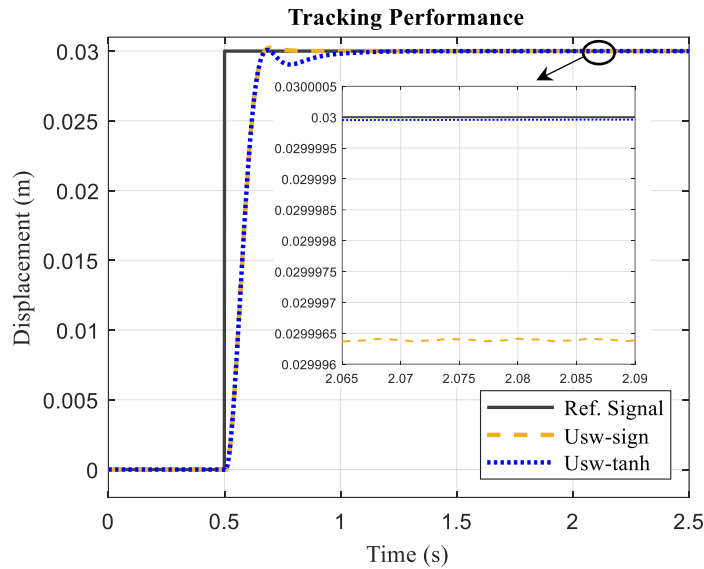


Fig. 4. The tracking performance of both switching functions.

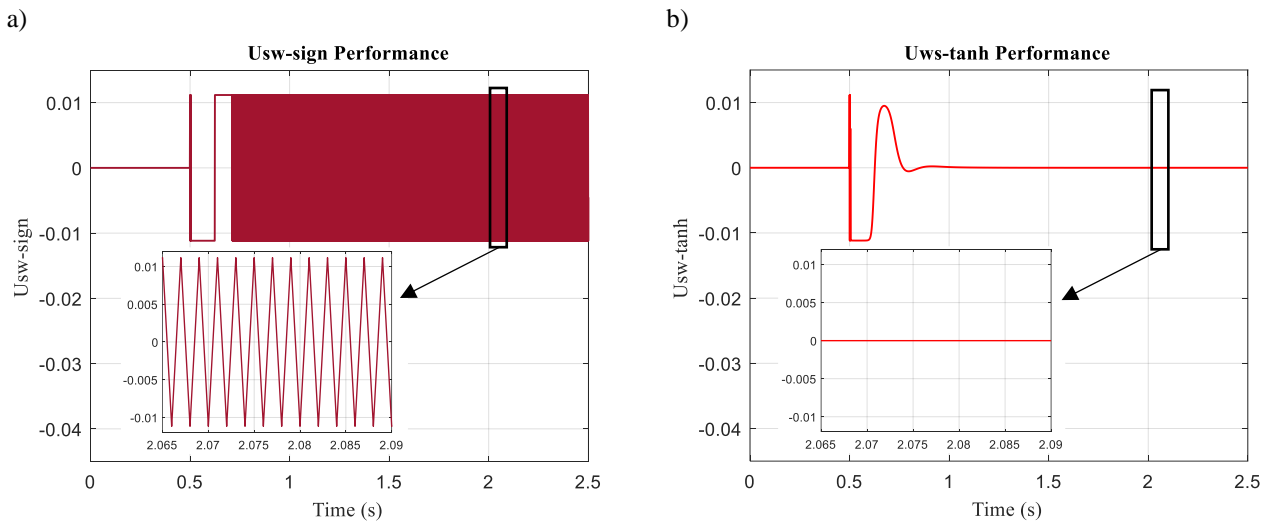


Fig. 5. The performance of different functions on switching control (a) signum function; (b) hyperbolic tangent function.

Further examination is conducted on the output of the switching function. As shown in the output performance of the signum switching function in Fig. 5(a), the chattering phenomenon has occurred. The effect somehow leads to the output tracking performance, as in Fig. 4. Chattering in real life is like a vibration that leads to wear and tear in a mechanical part.

When the hyperbolic tangent function is applied to the switching function, outstanding performance is obtained where the chattering phenomenon is greatly eliminated, as shown in Fig. 5(b). However, appropriate tuning with proper parameters is required to achieve this performance. The parameters as in Table I, as discussed in the previous section, implemented in the PSO algorithm shall obtain approximate parameters as in Table II.

## IV. CONCLUSION

The performances of both signum and hyperbolic tangent functions, implemented on the switching control of the sliding mode control (SMC), were examined. A great improvement can be achieved by applying the knowledge introduced by the mathematician, which also indicates the influence of mathematics on the world, especially in the engineering field. In this work, when the general signum function was substituted with the hyperbolic tangent function implemented on the switching function, outstanding performance was obtained where the chattering phenomenon was greatly eliminated—an uncomplicated manipulation in terms of mathematical reconstruction that lead to a major difference in the output performance.

## ACKNOWLEDGMENT

The support of Universiti Teknikal Malaysia Melaka (UTeM) is greatly acknowledged. The research was funded by UTeM Zamalah Scheme.

## REFERENCES

- [1] D. Zhang, D. Wang, Z. Xu, X. Zhang, Y. Yang, J. Guo, B. Zhang, and W. Zhao, "Diversiform sensors and sensing systems driven by triboelectric and piezoelectric nanogenerators," *Coord. Chem. Rev.*, vol. 427, pp. 1–15, 2021.
- [2] C. C. Soon, R. Ghazali, S. H. Chong, C. M. Shern, Y. M. Sam, and Z. Has, "Efficiency and performance of optimized robust controllers in hydraulic system," *Int. J. Adv. Comput. Sci. Appl.*, vol. 11, no. 6, pp. 385–391, 2020.
- [3] B. Guo, Z. Zhuang, J. S. Pan, and S. C. Chu, "Optimal Design and Simulation for PID Controller Using Fractional-Order Fish Migration Optimization Algorithm," *IEEE Access*, vol. 9, pp. 8808–8819, 2021.
- [4] V. Bharath Kumar, G. Charan, and Y. V. Pavan Kumar, *Design of robust pid controller for improving voltage response of a cuk converter*, vol. 661. Springer Singapore, 2021.
- [5] H. V. Puchta, Erickson Diogo Pereira and Bassetto, Priscilla and Biuk, Lucas Henrique and Itaborahy Filho, Marco Antonio and Converti, Attilio and Kaster, Mauricio dos Santos and Siqueira, "Swarm-Inspired Algorithms to Optimize a Nonlinear Gaussian Adaptive PID Controller," *Energies*, vol. 14, no. 12, pp. 1–20, 2021.
- [6] S. Ahmad, S. Ali, and R. Tabasha, "The design and implementation of a fuzzy gain-scheduled PID controller for the Festo MPS PA compact workstation liquid level control," *Eng. Sci. Technol. an Int. J.*, vol. 23, no. 2, pp. 307–315, 2020.
- [7] M. M. Gani, M. S. Islam, and M. A. Ullah, "Optimal PID tuning for controlling the temperature of electric furnace by genetic algorithm," *SN Appl. Sci.*, vol. 1, no. 8, pp. 1–8, 2019.
- [8] Y. G. Sun, J. Q. Xu, C. Chen, and G. Bin Lin, "Fuzzy H $\infty$  robust control for magnetic levitation system of maglev vehicles based on T-S fuzzy model: Design and experiments," *J. Intell. Fuzzy Syst.*, vol. 36, no. 2, pp. 911–922, 2019.
- [9] A. Das, U. K. Bera, and M. Maiti, "A solid transportation problem in uncertain environment involving type-2 fuzzy variable," *Neural Comput. Appl.*, vol. 31, no. 9, pp. 4903–4927, 2019.
- [10] A. K. Mishra, S. Das, and V. K. Yadav, "Finite-time synchronization of multi-scroll chaotic systems with sigmoid non-linearity and uncertain terms," *Chinese J. Phys.*, pp. 1–11, 2020.
- [11] X. Yang, X. Zhang, S. Xu, Y. Ding, K. Zhu, and P. X. Liu, "An approach to the dynamics and control of uncertain robot manipulators," *Algorithms*, vol. 12, no. 3, pp. 1–11, 2019.
- [12] C. C. Soon, R. Ghazali, S. H. Chong, C. M. Shern, Y. M. Sam, and A. A. Yusof, "Comparison of Fractional Order PID Controller and Sliding Mode Controller with Computational Tuning Algorithm," *Univers. J. Electr. Electron. Eng.*, vol. 6, no. 4, pp. 181–190, 2019.
- [13] C. C. Soon, R. Ghazali, C. S. Horng, C. M. Shern, Y. Sam, and A. A. Yusof, "Controllers Capabilities with Computational Tuning Algorithm in Nonlinear Electro-Hydraulic Actuator System," *J. Adv. Res. Fluid Mech. Therm. Sci.*, vol. 52, no. 2, pp. 148–160, 2018.
- [14] H. Maghfiroh, C. Hermanu, M. H. Ibrahim, M. Anwar, and A. Ramelan, "Hybrid fuzzy-PID like optimal control to reduce energy consumption," *Telkommika (Telecommunication Comput. Electron. Control.*, vol. 18, no. 4, pp. 2053–2061, 2020.
- [15] S. Mohammed, C. C. Soon, R. Ghazali, A. A. Yusof, Y. Md Sam, and C. Mau Shern, "An Electro-Hydraulic Servo with Intelligent Control Strategy," in *MATEC Web of Conferences*, 2018, vol. 150, pp. 1–5.
- [16] J. Li, J. Wang, H. Peng, Y. Hu, and H. Su, "Fuzzy-Torque Approximation-Enhanced Sliding Mode Control for Lateral Stability of Mobile Robot," *IEEE Trans. Syst. Man, Cybern. Syst.*, pp. 1–10, 2021.
- [17] Y. Xie, X. Zhang, W. Meng, S. Zheng, L. Jiang, J. Meng, and S. Wang, "Coupled fractional-order sliding mode control and obstacle avoidance of a four-wheeled steerable mobile robot," *ISA Trans.*, vol. 108, pp. 282–294, 2021.
- [18] S. Jung, "Improvement of Tracking Control of a Sliding Mode Controller for Robot Manipulators by a Neural Network," *Int. J. Control. Autom. Syst.*, vol. 16, no. 2, pp. 937–943, 2018.
- [19] A. Ma'arif and A. Çakan, "Simulation and arduino hardware implementation of dc motor control using sliding mode controller," *J. Robot. Control*, vol. 2, no. 6, pp. 582–587, 2021.
- [20] V. Nekoukar and N. Mahdian Dehkordi, "Robust path tracking of a quadrotor using adaptive fuzzy terminal sliding mode control," *Control Eng. Pract.*, vol. 110, no. 6, pp. 1–11, 2021.
- [21] H. Hassani, A. Mansouri, and A. Ahaitouf, "Robust autonomous flight for quadrotor UAV based on adaptive nonsingular fast terminal sliding mode control," *Int. J. Dyn. Control*, vol. 110, pp. 1–17, 2020.
- [22] K. B. Devika and S. Thomas, "Improved reaching law-based sliding mode controller for free flight autopilot system," *Int. J. Autom. Control*, vol. 12, no. 3, pp. 361–380, 2018.
- [23] A. Ş. Kaya and M. Z. Bilgin, "Output feedback control surface positioning with a high-order sliding mode controller/estimator: An experimental study on a hydraulic flight actuation system," *J. Dyn. Syst. Meas. Control. Trans. ASME*, vol. 141, no. 1, pp. 1–40, 2019.
- [24] Z. Xu, Z. Wang, Z. Shen, and Y. Sun, "Nonlinear differential and integral sliding mode control for wave compensation system of ship-borne manipulator," *Meas. Control (United Kingdom)*, vol. 54, no. 5–6, pp. 711–723, 2021.
- [25] Y. Cai, S. Zheng, W. Liu, Z. Qu, J. Zhu, and J. Han, "Sliding-mode control of ship-mounted Stewart platforms for wave compensation using velocity feedforward," *Ocean Eng.*, vol. 236, no. 7, pp. 1–11, 2021.
- [26] M. Ejaz and M. Chen, "Sliding mode control design of a ship steering autopilot with input saturation," *Int. J. Adv. Robot. Syst.*, vol. 14, no. 3, pp. 1–13, 2017.
- [27] T. Li, R. Zhao, C. L. P. Chen, L. Fang, and C. Liu, "Finite-time formation control of under-actuated ships using nonlinear sliding mode control," *IEEE Trans. Cybern.*, vol. 48, no. 11, pp. 3243–3253, 2018.
- [28] X. Zhou and X. Li, "Trajectory tracking control for electro-optical tracking system using eso based fractional-order sliding mode control," *IEEE Access*, vol. 9, pp. 45891–45902, 2021.
- [29] Y. Pan, C. Yang, L. Pan, and H. Yu, "Integral Sliding Mode Control: Performance, Modification, and Improvement," *IEEE Trans. Ind. Informatics*, vol. 14, no. 7, pp. 3087–3096, 2018.
- [30] C. C. Soon, R. Ghazali, H. I. Jaafar, S. Y. S. Hussien, S. M. Rozali, and M. Z. A. Rashid, "Optimization of Sliding Mode Control using Particle Swarm Algorithm for an Electro-Hydraulic Actuator System," *J. Telecommun. Electron. Comput. Eng.*, vol. 8, no. 7, pp. 71–76, 2016.
- [31] R. Ghazali, Y. M. Sam, M. F. Rahmat, C. C. Soon, H. I. Jaafar, and Zulfatman, "Discrete Sliding Mode Control for a Non-Minimum Phase Electro-Hydraulic Actuator System," in *2015 10th Asian Control Conference (ASCC)*, 2015, pp. 1–6.
- [32] C. C. Soon, R. Ghazali, H. I. Jaafar, and S. M. Hussein, Syarifah Yuslinda Syed Rozali, "Robustness Analysis of an Optimized Controller via Particle Swarm Algorithm," *Adv. Sci. Lett.*, vol. 23, no. 11, pp. 11187–11191, 2017.
- [33] M. Kalyoncu and M. Haydim, "Mathematical Modelling and Fuzzy Logic based Position Control of an Electrohydraulic Servosystem with Internal Leakage," *Mechatronics*, vol. 19, no. 6, pp. 847–858, 2009.
- [34] H. Xu, F. Fan, H. Zhang, Z. Le, and J. Huang, "A Deep Model for Multi-Focus Image Fusion Based on Gradients and Connected

Regions,” *IEEE Access*, vol. 8, pp. 26316–26327, 2020.

- [35] I. Eker, “Second-order Sliding Mode Control with Experimental Application,” *ISA Trans.*, vol. 49, no. 3, pp. 394–405, 2010.